

# Research on Solder Joint Quality Analysis Algorithm Based on Improved Deep Learning

Rui Wang<sup>1,2</sup>, Peng Wang<sup>1\*</sup>, Yaoyuan Wang<sup>2</sup>, Lidong Zhang<sup>2</sup>, Nan Chen<sup>2,3</sup>

<sup>1</sup>School of Computer Science and Technology, Changchun University of Science and Technology, Changchun 130022, Jilin, China

<sup>2</sup>Changchun College of Electronic Technology, Changchun 130012, Jilin, China

<sup>3</sup>College of Mechanical and Electrical Engineering, Changchun University of Science and Technology, Changchun 130022, Jilin, China

\*Corresponding Author.

## Abstract:

The quality of solder joints in circuit boards has a significant impact on the reliability of circuit operation. In order to improve the rapid detection ability of abnormal welding problems on the production line, different abnormal types are classified in a large number of inspection photos, and an improved deep learning-based solder joint quality analysis algorithm is proposed. First, the collected original image data is filtered to reduce the original noise. Then, through adaptive moment estimation and accelerated convolutional neural network, a large number of welding pictures are quickly classified to improve the processing speed. Finally, improved deep learning is used to complete the identification of solder joint quality. The experiment analyzes 6000 welding pictures, of which 4000 are training sets and 2000 are test sets. Compared with the traditional algorithm, the experimental results show that the recognition accuracy of the three algorithms is similar to more than 98% for small ball and bridge defects. For virtual solder and less tin defects, the recognition rates of the two traditional algorithms are 78.9% and 81.3%, respectively, while the algorithm is 93.5%, which has obvious advantages. In the test set of 2000 groups, the comprehensive detection rate and recall rate of this algorithm can reach 97.92% and 98.21%. This algorithm has a good application prospect in the process of quality inspection of a large number of solder joints of circuit boards.

**Keywords:** Solder joint quality identification, Deep learning, Detection rate, Identification parameters.

---

## I. INTRODUCTION

The effective application of intelligent detection technology is inseparable from machine vision, and the core of judgment through machine vision is the image recognition processing algorithm [1]. The welding forms of electronic product solder joints are different, and the welding degree requirements are also different. Therefore, it is difficult for traditional identification algorithms to meet the increasing testing needs. It is of great significance to develop algorithms with better identification capabilities. In order to realize the rapid identification of circuit board welding abnormalities, especially for high-integrated circuit boards with small components and high density, an accurate and fast image

recognition algorithm is the core of solving this problem. The welding abnormalities of traditional solder joints mainly include bridging, virtual soldering, small balls, solder beads, and voids [2-6]. Among them, problems such as small amount of solder, uneven solder joints, and unclear boundaries are difficult to identify.

In order to improve the detection effect of abnormal solder joints, a variety of image processing algorithms have been tried. Commonly used detection algorithms include: k-nearest neighbor classification algorithm, watershed algorithm, BP (Back Propagation) algorithm [7], deep learning algorithm [8], etc. The K-value nearest neighbor method [9] has a simple structure, but has low precision and weak nonlinear analysis ability. The watershed algorithm is suitable for small sample problems, but with the increase of the types of welding anomalies, its real-time performance is greatly reduced. The BP algorithm has a slow convergence speed and is prone to local extremes. The deep learning algorithm is one of the hottest application algorithms at present.

With the development of computer vision, intelligent control and pattern recognition, the application of deep learning-based image classification algorithms was born [10]. There have been studies on welding abnormality recognition abroad. Kazantsev et al. [11] proposed a small target recognition method based on non-parametric assumption statistics, and detected defects in specific areas. Lin DW [12] developed a computer vision detection algorithm to complete the detection of ship welding defects. Li et al. proposed an automatic seam recognition method using structured light vision, which improved the system environment adaptability [13]. Jiang HJ et al. [14] used the improved Sobel algorithm to realize the rapid detection of welding hole images. It can be seen that deep learning has the characteristics of strong recognition ability and fast speed, and has great advantages in welding quality image recognition. This paper proposes a welding image quality recognition algorithm based on deep learning, which has the advantages of high detection rate, low false detection rate and fast speed, which provides a new idea for the rapid detection of PCB welding defects.

## II. DATA PREPROCESSING BASED ON DEEP LEARNING

In order to be suitable for the requirements of quality identification of a large number of solder joints, the image collection needs to be preprocessed [15]. First, the grayscale histogram of the original image is converted to a uniform distribution, that is, the image above each grayscale has the same number of pixels, thereby achieving the effect of increasing the dynamic value range [16]. Assuming that the abscissa is the gray level of the image, the ordinate is the frequency of gray level pixels appearing in the image, and the range of the gray level  $k$  is  $[0, L-1]$ , then its gray histogram function is:

$$h(r_k) = n_k \quad (1)$$

Where  $r_k$  is the  $k$ -th gray level of the image, and  $n_k$  is the number of pixels with gray level  $r_k$  in the image.

Second, the grayscale value of each pixel in the image is modified point by point using the grayscale stretching algorithm. Let the original image be  $f(x, y)$  and its gray level range is  $[l_1, l_2]$ . In order to obtain an image  $g(x, y)$  with a grayscale range of  $[l_3, l_4]$ , the transformation functions that need to be used are

$$\frac{(T-l_3)(l_2-l_1)}{(l_4-l_3)(r-l_1)}=1 \quad (2)$$

Finally, in order to reduce the influence of stray noise due to uneven illumination of the background light and reflection interference on the surface of the PCB board in the process of welding image recognition, a smoothing algorithm is used to process the image, that is, noise reduction and filtering are used to improve the signal-to-noise of the welding image to be tested. Compare. In this system, the median filtering method is used to sort the corresponding values of all pixels and calculate the median  $Q_{mid}$ . After constructing the omnipotent matrix, the image can be expressed as:

$$g(i, j) = \sum_{(i,j) \in C} f(i, j) \cdot TQ_{mid} \quad (3)$$

In the formula,  $(i, j)$  represents the pixel position, and  $(i, j) \in C$  is within the boundary  $C$  of the welding image. Since the gray value of the central pixel is determined according to the statistical classification results of the gray value of the original central pixel and its surrounding pixels, this filtering algorithm is suitable for nonlinear image processing. Using median sorting can easily exclude isolated pixels such as high-brightness noise with little impact on the overall image, thus greatly reducing the interference of discrete noise in the image on image quality.

### III. IMPROVED DEEP LEARNING ALGORITHM

Deep learning itself has good classification characteristics, but the selection of parameters has a significant impact on the classification effect, so improving it will get better classification results [17]. The input samples can be preliminarily processed using a convolutional neural network. This algorithm designs an improved deep learning algorithm with 5 layers, including input layer, convolution layer, pooling layer, connection layer and classification layer.

In the convolutional layer of this system, the convolution operation is performed by a convolution kernel whose three indicators are length, width and depth. The convolution operation can be expressed as:

$$S(i, j) = \sum_x \sum_y I(x, y)K(i-x, j-y) \quad (4)$$

In the formula,  $I$  represents a two-dimensional image, and  $K$  represents a two-dimensional convolution kernel.  $x$  and  $y$  represent the position of a corresponding pixel in the range of  $i$  and  $j$ , respectively, and the area of the set of  $x$  and  $y$  represents the solder joint area. For each pixel in the image, the adjacent pixels and the corresponding pixels of the convolution kernel are multiplied and summed, that is, the pixel value

of the point is obtained, that is, the forward propagation of the convolutional neural network. Convolutional neural networks are forward neural networks, and the training samples do not need to be too large. Therefore, it has good compatibility with different defect types of a large number of welding images. The network structure consists of input layer, convolution layer, dimension reduction layer, connection layer and output layer. After the welding image enters the output layer, it is convolved with the kernel function, and the result is the output neuron of the excitation function, which realizes the acquisition of the feature image and enters the next layer. Let the  $j$ th feature of the  $n$ th convolutional layer be

$$\begin{cases} X_j^n = f \left[ \sum_{i=0, j=0}^n (X_i^{n-1} \times k_{i,j}^n) + b_j^n \right] \\ Y_j^n = f \left[ \eta g Y_j^{n-1} + b_j^n \right] \end{cases} \quad (5)$$

In the formula,  $f()$  is the excitation function,  $N_j$  is the upper-layer feature image set,  $k_{i,j}^n$  is the convolution kernel weight, and  $b_j^n$  is the sum bias. After acquiring the features, import the dimension reduction layer to reduce the amount of computation.  $g()$  is the dimensionality reduction function,  $\eta$  is the product bias, and  $b_j^n$  is the sum bias.

Because of the diversity of abnormal welding image features, although there are similarities in each defect, the size and shape of each defect are still quite different, so it is necessary to have the adaptability of data selection. Improvements Convolutional Neural Networks was designed. When the input data sample is  $\{x_i^p\} (p=1,2,\dots,m, i \text{ is the component})$ , and the output is  $C_{ij}$ , there are

$$C_{ij} = \sigma \left\{ \sum_{i=1}^n [\eta(C_{ij})(x_i^p - \omega_j)] x_i^p \right\} \quad (7)$$

Among them,  $\sigma()$  is a monotonic function, and  $\omega_j$  is the weight of the  $j$ -th neuron. The output layer thus obtained is equivalent to sample data with a central distribution, and the training network and the learning network can cooperate to achieve accelerated convergence.

#### IV. ALGORITHM IMPLEMENTATION

After filtering and denoising the original data, a good image classification and recognition ability can be obtained through a 5-layer deep learning network. According to the improved deep learning algorithm, the data flow chart based on the deep convolutional neural network model is designed, as shown in Fig 1.

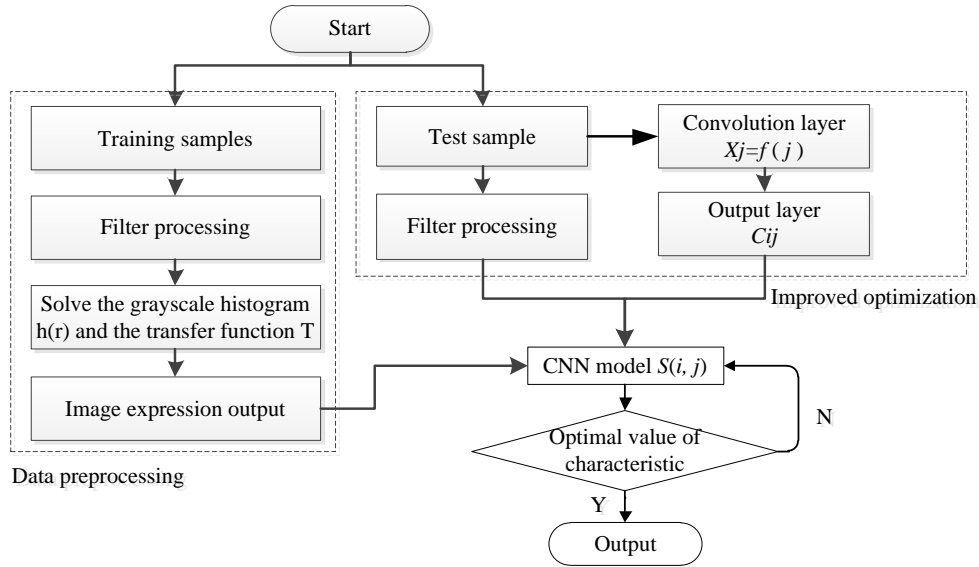


Fig 1: Improved deep learning algorithm flowchart

As shown in Fig 1, the input data is divided into two groups, one for training sample analysis and one for testing sample analysis. In the training set, the quantitative classification of the data is completed by computing the gray histogram function  $h(r)$  and the transfer function  $T$ . The image representation output is then imported into the CNN network [18-20]. The test dataset will also be imported into the CNN network after filtering and denoising the data. In addition, the test set data will also solve the control parameters of the corresponding correlation layer ( $X_i$ ) and output layer ( $C_{ij}$ ), so as to jointly control the total amount of imported data. Finally, the iteration of the image data is completed in the CNN model, and the classified test data is output after the iteration is completed. Cross Entropy is used as the loss function in the algorithm. In the process of network model training, because the traditional stochastic gradient descent method is easy to fall into the problem of local optimum, this algorithm adopts the adaptive adjustment method to complete the learning of each model parameter. The adaptive moment estimation algorithm is used as a back-propagation optimization algorithm to accelerate the training of convolutional neural networks, thereby improving the training accuracy. During this process, the gradient mean and variance are continuously corrected to make the iterative average calculation more accurate.

## V. EXPERIMENTS

### 5.1 Hardware Conditions

In the experiment, the welding image was acquired by the X-ray emitter and 2000-CCD [21]. The welding pictures include 5 different situations such as virtual soldering, small balls, connecting bridges, and less tin. Due to the different types of circuit boards, the brightness and contrast of the images are obviously different, so in the image preprocessing, all of them are first adjusted to a similar grayscale range. Among them, 4000 images are used as training set, 1000 images are used as validation set, and the last 1000 images are used as test set. The test system is shown in Fig 2

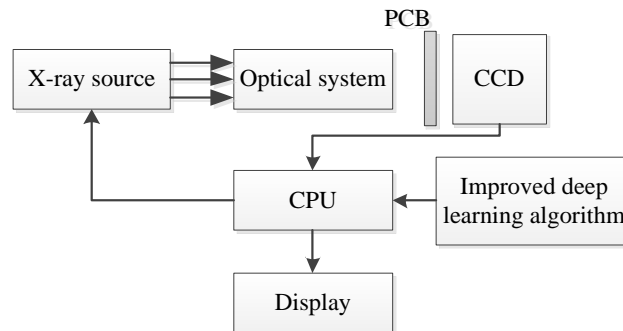
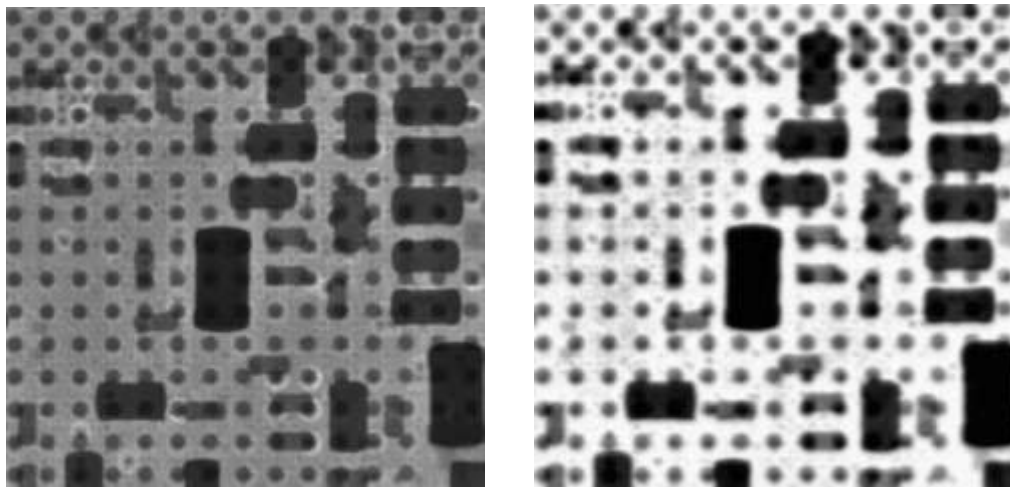


Fig 2: Test system structure diagram

In a solder joint quality inspection system, it is desirable to satisfy both a high detection rate and a low false detection rate. The detection rate refers to the detection of solder joints and seams that have welding problems; the false detection rate refers to the percentage of defective images that are incorrectly detected as normal images to the total number of defective images. The solder joint quality detection algorithm based on deep learning is completed in the Linux system, and the hardware configuration is NF5820M5 server and Xeon-3110 CPU. It is implemented in Python language under the Tensorflow system.

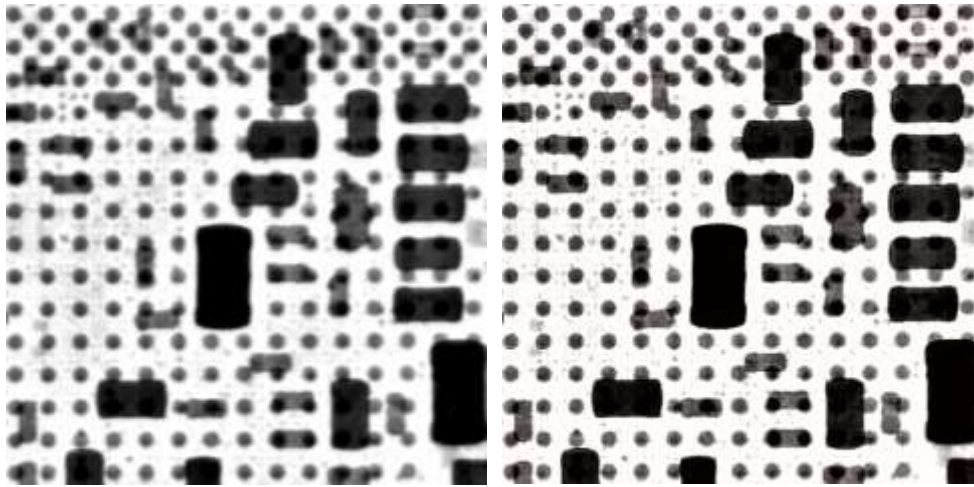
### 5.2 Optimization Analysis of Solder Joint Images

In order to verify the effectiveness of the proposed deep learning-based solder joint image extraction algorithm, this paper compares the algorithm with the k-nearest neighbor classification algorithm and the watershed algorithm. The test was conducted with pictures of circuit boards containing five solder defects. The image effects obtained using the three algorithms are shown in Fig 3.



(a) The original image

(b) k-nearest neighbor classification algorithm



(c) watershed algorithm

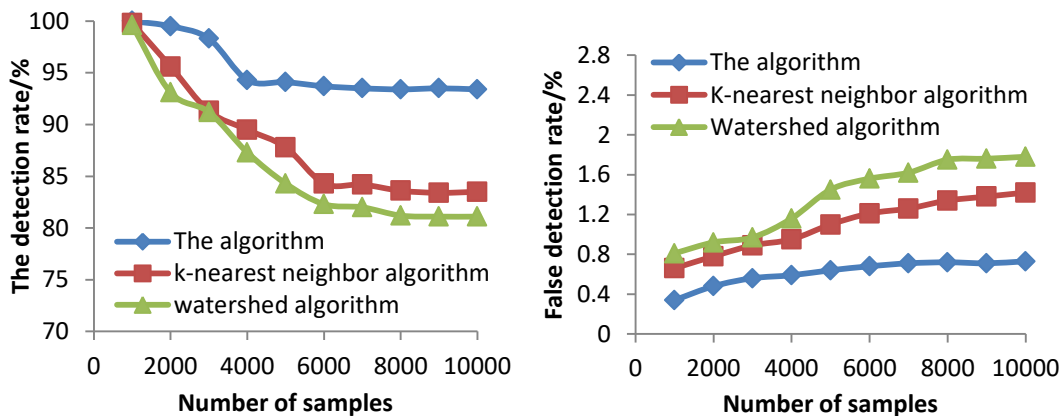
(d) this algorithm

Fig 3: Different algorithm processing results

The test results show that the Canny edge detection and segmentation algorithm has the best effect on the boundary definition of each solder joint in the processed image. The gradient and clarity of this algorithm are better for details such as solder thickness and bias in the solder joints. It can be seen from the three sets of images that the lack of solder, small balls and bridges are very obvious, as long as the corresponding algorithm can be directly extracted and counted. The situation is different, such as false soldering, partial ball, less tin, etc. It is necessary to perform deep information mining on the image, otherwise it is difficult to identify or easy to cause misjudgment.

### 5.3 Performance Analysis

In order to further verify the advantages of this algorithm, all the last 1000 test set pictures are input into the three algorithms for iterative identification, and statistical analysis is carried out after the classification is completed. The detection rate and false detection rate are statistically analyzed, and the statistical results are shown in the Fig 4 shown.



(a) The detection rate

(b) false detection rate

Fig 4: Algorithm performance analysis

It can be seen from Fig 4(a) that the detection probability of the three algorithms is close to 99.5% when the total amount of data is 1000, but as the amount of data continues to increase, the detection rate of the two compared methods gradually decreases, exceeding 6000. After that, it was basically stable at 83.6% and 81.2%. The convergence speed of this algorithm is faster, and it is stable at 93.5% at about 5000 sheets. It can be seen that the detection rate of this system is relatively less affected by the total amount of test samples. It can be seen from Fig 4(b) that the false detection rates of the three algorithms are 0.34%, 0.66% and 0.081% respectively when the total amount of data is 1000. With the increase of the amount of data, the false detection rate of the two compared methods increases obviously, reaching 1.42% and 1.78% respectively when the number of images is 10,000. At this time, the false detection rate of this algorithm is only 0.73%. And the change curve of the false detection rate of this algorithm is smoother, which means that the fitting of the algorithm is better. It can be seen that the detection rate of this system is relatively less affected by the total number of test samples. In short, the comprehensive detection rate and false detection rate of this algorithm have been improved to some extent.

#### 5.4 Analysis of Accuracy of Defect Type Recognition

In order to analyze the recognition accuracy of the algorithm for different defect types, the experiments identify defects in a large number of different types of welding images with welding quality problems, including small balls, virtual welding, eccentricity, less tin and bridges. After training through the deep learning model, the average recognition accuracy of various welding quality defect images is shown in Fig 5.

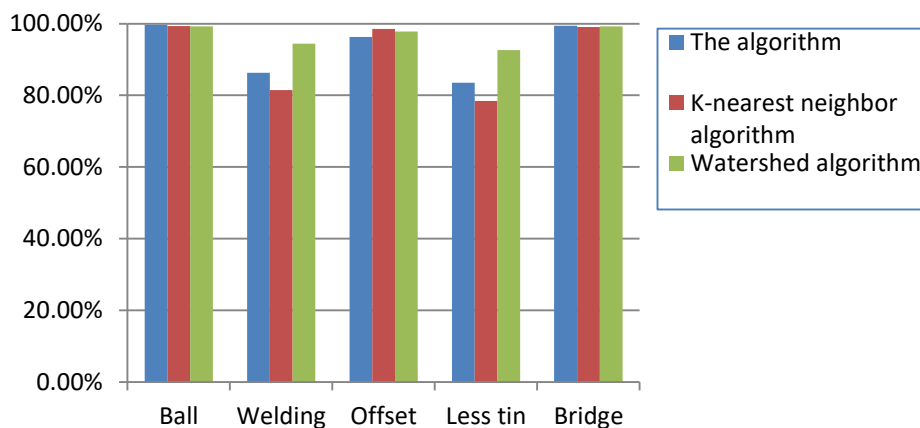


Fig 5: Comparison of detection results of different algorithms

As shown in Fig 5, the images obtained by the three methods can clearly distinguish defects caused by small balls and bridges, and the detection rate is better than 99.5%; in the detection of partial ball defects, the detection rate of the k-nearest neighbor classification algorithm higher, reaching 98.6%, while the watershed algorithm and this algorithm are 96.4% and 97.7% respectively. The analysis shows that its boundary extraction accuracy is high, which makes it have higher accuracy in spherical size and shape analysis; in the detection of virtual welding defects, the effect of this algorithm is the best, the detection



rate is 94.3%, while the k-nearest neighbor classification algorithm and the watershed algorithm are 86.4% and 80.8% respectively; in the detection of less tin defects, the effect of this algorithm is the best, the detection rate is 92.5% %, while the k-nearest neighbor classification algorithm and the watershed algorithm are 83.4% and 78.2% respectively; the analysis believes that the reason for the obvious decrease in the detection effect of the latter two defects is that: for the watershed algorithm, in order to obtain better edges, the details of the solder joints are The grayscale smoothing is too large, which reduces the detail information, so the detection rate drops significantly; and the k-nearest neighbor classification algorithm may cause some selected points to overlap with image noise due to the randomness of the K value, resulting in improper initial value settings, thus affecting the classification. Effect. The experimental results show that, compared with the traditional image segmentation algorithm, this algorithm can better obtain various welding defect images, thus providing better support for welding quality analysis.

### 5.5 Algorithm Stability Analysis

Three algorithms are used to iteratively approximate the optimal solution, so as to analyze the variation law of the maximum fitness of the three methods. The results are shown in Fig 6.

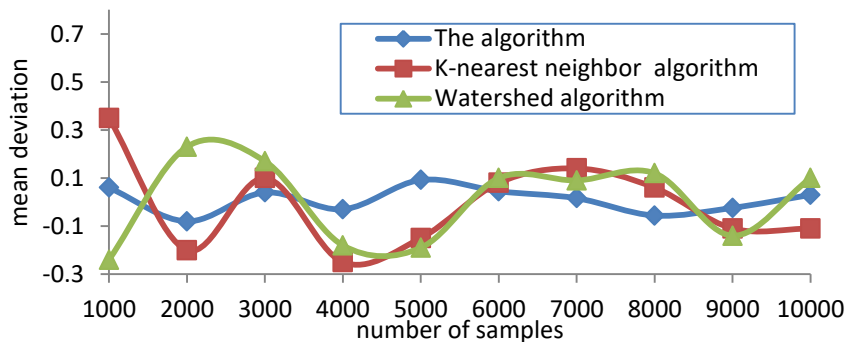


Fig 6: Comparison of the stability of the three algorithms

It can be seen from Fig 6 that with the increase of the number of iterations, the maximum fitness values of the three algorithms will tend to be stable, but in contrast, the algorithm is basically stable after more than 2000 times, while the k-nearest neighbor classification algorithm and The watershed algorithm tends to be stable at 3000 and 4000 times respectively, which shows that the stability of this algorithm is better than that of the traditional algorithm. The larger the number of samples in the iterative process, the more stable the mean error. Comparing the mean deviation of the three algorithms, it can be seen that the mean deviation of this algorithm is more concentrated and smaller.

## VI. CONCLUSIONS

This paper proposes a welding image quality recognition algorithm based on deep learning, which combines a large number of welding spot welding images for training and verification, and achieves the needs of improving the test speed and reducing the false detection rate. Through experiments to identify

and detect a large number of welding images, and compared with the traditional algorithm, the results show that the comprehensive detection rate, false detection rate and recall rate of this algorithm are better than the traditional algorithm, which verifies that it can provide rapid detection of circuit board defects, better technical support.

## REFERENCES

- [1] Shah H N M, Sulaiman M, Shukor A Z, et al. Butt welding joints recognition and location identification by using local thresholding, *Robotics and Computer-Integrated Manufacturing*, 2018, 51:181-188.
- [2] Ma Jiangli. Research on Art Appraisal Based on Hyperspectral Imaging Technology, *Cultural Relics Protection and Archaeology*, 2018, 30(03):15-19.
- [3] Zuo Kezhu, Zou Yuanyuan, Li Pengfei, et al. Iterative based identification method for boundary feature points of unequal thickness laser tailor welded seams, *Journal of Applied Lasers*, 2018, 38(03): 114-119.
- [4] Fu Li. Application of High Temperature Laser Welding Innovation Technology to Expand Advanced High Strength Steel, *Aerospace Manufacturing Technology*, 2018(1): 70-70.
- [5] Kazantsev I G, Lemahieu I, Salov G I, et al. Statistical detection of defects in radiographic images in nondestructive testing, *Signal Processing*, 2002, 82(5):791-801.
- [6] Hu Haiying, Hui Zhenyang, Li Na. Airborne LiDAR Point Cloud Classification Based on Multiple-Entity Eigenvector Fusion, *Chinese Journal of Lasers*, 2020, 47(8):229-239.
- [7] Muhammad J, Altun H, Abo-Serie E. Welding seam profiling techniques based on active vision sensing for intelligent robotic welding, *The International Journal of Advanced Manufacturing Technology*, 2017, 88(1-4):127-145.
- [8] Qiang G, Shanshan Z, Yang Z, et al. Detection Method of PCB Component Based on Automatic Optical Stitching Algorithm, *Circuit World*, 2015, 41(4):133-136.
- [9] Garcia-Pineda O, MacDonald IR, Li X, et al. Oil Spill Mapping and Measurement in the Gulf of Mexico with Textural Classifier Neural Network Algorithm (TCNNA), *IEEE Journal of Selected Topics in Applied Earth Observations and Remote Sensing*, 2013, 6(6): 2517-2525.
- [10] Richardson Michael L, Ojeda Patricia I. A "Bumper-Car" Curriculum for Teaching Deep Learning to Radiology Residents, *Academic Radiology*, 2022, 29(5): 763-770.
- [11] Liu Y, Yu F. Automatic Inspection System of Surface Defects on Optical IR-CUT Filter Based on Machine Vision, *Optics and Lasers in Engineering*, 2014, 55: 243-257.
- [12] Yesilbudak M, Sagiroglu S, Colak I. A New Approach to Very Short Term Wind Speed Prediction Using K-Nearest Neighbor Classification, *Energy Conversion and Management*, 2013, 69:77-86.
- [13] Sreejini K S, Govindan V K. Improved multi-scale matched filter for retina vessel segmentation using PSO algorithm, *Egyptian Informatics Journal*, 2015, 16: 253-260.
- [14] Baraldi P, Cannarile F, Maio F D, et al. Hierarchical k-nearest neighbors classification and binary differential evolution for fault diagnostics of automotive bearings operating under variable conditions, *Engineering Applications of Artificial Intelligence*, 2016, 56:1-13.
- [15] Issac A, Sarathi M P, Dutta M K. An adaptive threshold based image processing technique for improved glaucoma detection and classification, *Computer Methods and Programs in Biomedicine*, 2015, 122(2): 229-244.
- [16] Wang Haijun, Kong Xiangdong, Zhang Bo. The simulation of lucc based on ogistic-CA -Markov model in Qilian Mountain area, *Sciences in Cold and Arid Regions*, 2016, 8(4):350-358.
- [17] Zhang Jun. Identification of weld defects based on principal component analysis, *Industrial Control Computer*, 2017, (01): 111-112.

- [18] Wei Heng, Lu Lin, Pu Tao, et al. Fiber time delay fluctuations measurement based on one-way transfer, *Infrared and Laser Engineering*, 2020, 49(8): 176-181.
- [19] Ahmadian Sajad, Ahmadian Milad, Jalili Mahdi. A deep learning based trust- and tag-aware recommender system, *Neurocomputing*, 2022, 488: 557-571.
- [20] Wang Guo, Wang Cheng, Zhang Zhenxin, et al. Single tree segmentation method of urban distributing belt based on vehicle-borne laser point cloud data, *Laser & Infrared*, 2020, 50(11):1333-1337.
- [21] Sun Xu, Li Xiaoguang, Li Jiafeng, et al. Research progress of image super-resolution restoration based on deep learning, *Acta Automatica Sinica*, 2017, 43(5): 697-709.